OPTIMAL FEEDBACK CONTROL OF MICROVIBRATIONS

G. S. Aglietti[1], E. Rogers[1], J. Stoustrup[2], R. S. Langley[3], and S. B. Gabriel[1]

[1]University of Southampton, U.K.
[2]Aalborg University, Denmark.
[3]University of Cambridge, U.K.

ABSTRACT

The performance of sensitive equipment such as microgravity experiments or accurately targeted optical instruments can be seriously degraded by vibrations produced by other equipment mounted on the same supporting structure, eg a spacecraft. Also it is well known that active control must be used in order to suppress the effects of low amplitude vibrations in the range up to 1 KHz which are termed microvibrations. In this paper we describe a systematic technique for modeling the dynamics of a generic structure subject to microvibrations. This produces a finite dimensional approximate model in linear state space form which is then used to compare the performance of linear quadratic optimal control algorithms in this general area.
Keywords: microvibrations, active control.

1 INTRODUCTION

Sensitive equipment often has to be mounted on structures where vibrations induced by the functioning of other necessary pieces of equipment mounted on the same underlying structure can produce unacceptably high degradation of performance. This situation is very common onboard spacecraft [1], where, for example, microrgravity experiments or accurately targeted optical instruments are frequently mounted on panels where reaction wheels, crycoolers, etc act as vibration source(s).

In practice, the reduction of the vibration level by passive means (termed passive control) in a structure can be attempted by action at the source(s), receiver(s), and along the vibration path(s). At the source(s), this action consists of attempting to minimize the amplitude(s) of the vibration(s) by, for example, placing equipment on appropriate mountings. The same approach is very often used at the receiver(s) but with the basic objective of sensitivity reduction. Finally, along the vibration path(s), modifications of structural elements or re-location of equipment is attempted with the aim of reducing the mechanical couplings between source(s) and receiver(s).

All of the above approaches are based on so-called passive damping technology and, for routine applications, an appropriate combination of them is often capable of producing the desired levels of dynamic disturbance rejection. The use of active control schemes in such cases would only be as a last resort to achieve desired performance. In the case of microvibrations, taken to be low amplitude vibrations which occur at frequencies in the range up to 1 KHz, only active control can be expected to provide the required level of vibration suppression.

To investigate the use of active control to suppress microvibrations in a structure, computationally feasible models which retain the core features of the underlying dynamics are clearly required. The most obvious approach to the development of such models is to use finite element methods (FEM) (see, for example, the discussion of this point in [1]) due to the accuracy available with a sufficiently fine mesh. The only difficulties with such an approach are the computational intensity of the models and the fact that they are not in a form compatible with feedback control systems design. They can, however, be used, as here, to verify that an alternative modeling strategy produces realistic model on which to base controller design and evaluation.

Alternatives to FEM can be classified as elastic wave methods, variational methods, and impedance based methods respectively. A detailed study of the advantages and disadvantages of these methods, together with background on each of them, can again be found in [1]. Based on this study, a Lagrange-Rayleigh-Ritz (LRR) method whose development is detailed in [1, 2, 3] is used to produce the mathematical models for the controller design studies reported in this paper.

These studies take the form of a comparative investigation into the performance of controllers based on linear quadratic optimal control theory applied to equipment mounted on a panel which is known to be a realistic basis to undertake initial studies of this kind. The actuators and sensors used are of the piezoelectric variety which are currently the subject

of much interest for control systems implementation in many different applications domains. In the next section we summarize the required background with complete details in [1, 2, 3].

2 MODELING

Modeling equipment mounted on a panel is most easily undertaken by assuming lumped masses. If, however, the equipment itself has dynamics then the lumped mass approximation is no longer valid and a more detailed representation of the mounting geometry needs to be considered. In which case, first note that each particular piece of equipment could have a different mechanical interface securing it to the structure underneath. By far the most common mounting geometry is four feet positioned at its corners as illustrated in Figure 1. The mounting feet, in the form of piezoelectric patches, are the actuators for control at a source or at a receiver, and piezoelectric patches bonded onto the panel are the sensors/actuators for control along the structure.

The model of the complete plant (or process) here is constructed by assembling together the model of the actively controlled panel and the model of the equipment on their suspension systems. In this case, the sub-system models (the panel and the equipment on their suspension systems) are both derived using Lagrange's equations of motion, i.e.

$$\frac{d}{dt}(\frac{\partial\, T}{\partial\, \dot{q}_i}) - \frac{\partial\, T}{\partial\, q_i} + \frac{\partial\, U}{\partial\, q_i} = Q_i \tag{1}$$

where T and U respectively denote the total kinetic and potential energy in the system respectively, q_i is the ith generalized co-ordinate, and Q_i is the ith generalized force. Hence the task now is to find expressions for the kinetic and potential energies of each sub-system.

Consider first the panel and let the subscript pl refer to the panel and pz to the piezoelectric patches. Then we have that

$$\begin{aligned} T &= T_{\rm pl} + T_{\rm pz} \\ U &= U_{\rm pl} + U_{\rm pz} \end{aligned} \tag{2}$$

Also the displacement field (out-of-plane displacement w) is described as a superposition of shape functions $S_{m,n}$ (consisting of the modes of the bare panel), multiplied by $\psi_{m,n}(t)$ which denotes time dependent modal co-ordinates, i.e.

$$\begin{aligned} w(x,y,t) &= \sum_{m=1}^{Nm}\sum_{n=1}^{Nn} S_{m,n}(x,y)\psi_{m,n}(t) \\ &= s^T\Psi \end{aligned} \tag{3}$$

where s is the vector of shape functions and Ψ is the vector of modal co-ordinates.

In the application of Lagrange's equations here, the full set of generalized co-ordinates q_i is composed of Ψ and the voltages at the piezoelectric patches. The excitation considered (in its most general form) is modeled as N_f point forces F_j acting at arbitrary locations on the panel. Hence the generalized forces in (1) will have the form

$$Q_i = \sum_{j=1}^{N_f} F_j \frac{\partial\, w}{\partial\, f_i} \tag{4}$$

or $Q = S_f f$ where f is the vector of forces and S_f is a matrix containing the modal shape vector s evaluated at the force locations.

The kinetic energy terms which form T of (1) can be calculated directly by integration using the standard formula

$$T = \frac{1}{2}\int\int\int_{\rm Vol} \rho \dot{w}^2\; dx\; dy\; dz \tag{5}$$

where ρ is the material density. This yields (see [1] for the details)

$$\left.\begin{aligned} T_{\rm pl} &= \tfrac{1}{2}\dot{\Psi}^T M_{\rm pl}\dot{\Psi} \\ T_{\rm pz} &= \tfrac{1}{2}\dot{\Psi} M_{\rm pz}\dot{\Psi} \end{aligned}\right\} \tag{6}$$

where $M_{\rm pl}$ is the (diagonal) inertia matrix of the bare panel and $M_{\rm pz}$ is the (fully populated) inertia matrix defined, in effect, by evaluating (5) over the total number of patches used. The off-diagonal terms in this last matrix represent the coupling between the modal co-ordinates.

The potential energy of the panel is obtained by evaluating the integral

$$U = \frac{1}{2}\int\int\int_{\rm Vol} \epsilon^T\sigma\; dx\; dy\; dz \tag{7}$$

where ϵ and σ are the strain and stress vectors respectively. By assuming a plane stress condition for the panel we can write (7) in the form

$$U_{\rm pl} = \frac{1}{2}\Psi^T K_{\rm pl}\Psi \tag{8}$$

where $K_{\rm pl}$ is the so-called stiffness matrix.

In the case of the piezoelectric patches, their potential energy can be expressed as the sum of three components

$$U_{\rm pz} = U_{\rm pz}^{\rm elast} + U_{\rm pz}^{\rm elastelect} + U_{\rm pz}^{\rm elect} \tag{9}$$

where

$$\left.\begin{aligned} U_{\rm pz}^{\rm elast} &= \tfrac{1}{2}\Psi^T K_{\rm pz}^{\rm elast}\Psi \\ U_{\rm pz}^{\rm elastelect} &= \tfrac{1}{2}v^T K_{\rm pz}^{\rm elastelect}\Psi \\ U_{\rm pz}^{\rm elect} &= \tfrac{1}{2}v^T K_{\rm pz}^{\rm elect} v \end{aligned}\right\} \tag{10}$$

and v is the column vector of voltages at the piezoelectric patches. As before the matrices in (10) can be computed using known formulas [1].

Given these terms, suppose some of the patches are employed as actuators and the rest as sensors, let v_a and v_s be the corresponding voltage vectors, and let $K_{\rm pza}^{\rm elastelect}$ and $K_{\rm pzs}^{\rm elastelect}$ denote the corresponding partitions of the matrix $K_{\rm pz}^{\rm elastelect}$. Then application of (1) yields the following model for Ψ

$$M_{\rm acp}\ddot{\Psi} + C_{\rm acp}\dot{\Psi} + K_{\rm acp}\Psi = H \tag{11}$$

where damping has been introduced via the matrix $C_{\rm acp}$, and

$$H = V_a v_a + S_f f \tag{12}$$

Also

$$v_s = H_1 \Psi \tag{13}$$

The matrices in (11)-(13) are not detailed here for brevity but, see [1, 2, 3] for the details, can be directly computed from the panel dimensions and properties and the energy terms.

The above procedure can be extended to model the dynamics of the pieces of equipment mounted on the panel (as illustrated in Figure 1). Each enclosure here is assumed to have three degrees of freedom (dof's), i.e. out-of-plane displacement, pitch angle, and roll angle respectively which are written in vector form as $\Psi_{\rm eqp}$. This particular choice of dof's allows us to express the kinetic energy associated with any piece of equipment as

$$T_{\rm eqp} = \frac{1}{2}\dot{\Psi}_{\rm eqp}^T M_{\rm eqp}\dot{\Psi}_{\rm eqp} \tag{14}$$

where $M_{\rm eqp}$ is the associated inertia matrix.

The potential energy associated with the equipment is, in effect, the sum of that stored in the flexible supporting elements. This energy can be evaluated as the sum of the elastic energy, the elastoelectric energy and the electric energy stored in each mounting foot. Next we outline the development of a representation for each of these energies with full details in [3].

The elastic energy stored in each suspension, which consists of a stiffness, dashpot and piezoelectric prism connected in parallel, is proportional to the square of the linear deformation $\Delta z_i, 1 \le i \le 4$, of the ith mounting foot and this deformation is given by the difference between the out-of-plane displacement of the panel surface ($w(x, y, t)$) evaluated at the mounting foot location (x_i, y_i) and the vertical displacement ($z_i(t)$) of the ith corner of the box. Suppose also that $\Psi_c = \left[\Psi^T, \Psi_{\rm eqp}^T\right]^T$. Then the total (i.e. for all four mounting feet) elastic energy can be written as

$$U_{\rm eqp}^{\rm elast} = \frac{1}{2}\Psi_c K_{\rm eqp}^{\rm elast}\Psi_c \tag{15}$$

Consider now one of the piezoelectric prisms used in the mounting feet suspensions of height h_{pz} with a voltage v_i applied across the electrodes on the top and bottom faces. Then a constant electric field $e = \frac{v_i}{h_{pz}}$ acting in an axial direction can be assumed in the material which has Young's modulus E_{pz} and piezoelectric constant d_{zz}. The stress produced along the same axial direction will therefore be constant and related to the applied voltage by the equation

$$\sigma_{\rm elect_i} = E_{pz} d_{zz} \frac{v_i}{h_{pz}} \tag{16}$$

Also the strain in the material can be assumed constant and given by

$$\epsilon_{z_i} = \frac{\Delta z_i}{h_{pz}} \tag{17}$$

and the elastoelectric energy stored in each piezoelectric stack used can be computed by application of a standard formula.

Suppose now that the column vector $v_{\rm eqp}$ denotes the voltages v_i across the electrodes in the mounting feet used. Then the total elastoelectric energy stored in the equipment suspension system can be written as

$$U_{\rm eqp}^{\rm elastoelect} = \frac{1}{2} v_{\rm eqp}^T K_{\rm eqp}^{\rm elastoelect} v_{\rm eqp} \tag{18}$$

Assuming a uniform electric field exists across the piezoelectric prisms, the electric energy studied in each of them is given by $\frac{1}{2}Cv_i^2$ where C is the capacitance of the prisms. Hence the total stored electric energy can be expressed as

$$U_{\rm eqp}^{\rm elect} = \frac{1}{2} v_{\rm eqp}^T K_{\rm eqp}^{\rm elect} v_{\rm eqp} \tag{19}$$

In this case, the 4×4 matrix involved is diagonal with each element equal to C.

The presence of dissipative forces produced by the dashpots in the mounting feet means that an extra term must be added to the generalized forces in (1) applied to this case. This extra term, denoted by $Q_{\rm dp}$, is proportional to $\Delta\dot{z}_i$ and can be written as

$$Q_{\rm dp} = C_{\rm dp}\dot{\Psi}_e \tag{20}$$

where $C_{\rm dp}$ includes the contribution of each foot. It is also necessary to take account of the internal dynamics of the pieces of equipment. This is achieved by adding an extra dof to $\Psi_{\rm eqp}$ with associated mass and stiffness added to $M_{\rm eqp}$ and $K_{\rm eqp}^{\rm elast}$.

To apply (1) to obtain the final model of the overall system composed of the actively controlled panel and, say, Ne pieces of equipment mounted on it, the

generalized co-ordinate is taken (with obvious notation on the right-hand side) to be

$$r = \left[\Psi^T, \Psi_{eqp_1}^T, \cdots, \Psi_{\mathrm{eqp}_{N_e}}\right]^T \tag{21}$$

Also introduce (again with obvious notation on the right-hand side)

$$v_e = \left[v_{\mathrm{eqp}_1}^T, \cdots, v_{\mathrm{eqp}_{N_e}}^T\right]^T \tag{22}$$

Suppose also that all stiffness and mass matrices associated with (i) the actively controlled panel and the pieces of equipment, and (ii) those associated with the actuators of the suspensions, have been augmented with rows and columns of zeros to be compatible with the dimension of r. Then on application of (1) the motion of actively controlled structure can be written as

$$M_{\mathrm{acs}}\ddot{r} + C_{\mathrm{acs}}\dot{r} + K_{\mathrm{acs}}r = H_1 \tag{23}$$

where

$$H_1 = V_e v_e + V_a v_a + Sf \tag{24}$$

These last two equations govern the motion of the actively controlled structure excited by external sources (f),voltage inputs at the active suspensions (v_e), and the piezoelectric patches acting as actuators (v_a). Once the solution r is available, the displacement at any point on the panel can be obtained from

$$w = \left[s^T, 0\right] r \tag{25}$$

and the displacements of the equipment enclosures are simply the corresponding elements in r. In the case when the vibration levels of the actively controlled equipment have to be monitored, these are easily inferred from the function dof's.

3 CONTROLLER DESIGN

For a given arrangement, the model construction of the previous section can be implemented in MATLAB to directly produce (via (24) and (25)) a state space model of the following form on which to base controller design

$$\begin{aligned} \dot{x} &= Ax + B_1 v + B_2 f \\ v_s &= C_v x \\ w_{out} &= C_w x \end{aligned} \tag{26}$$

where, in particular, $x = \left[r^T \dot{r}^T\right]^T$, $v = \left[v_e^T v_a^T\right]^T$ and the observed and controlled output matrices C_v and C_w are defined by

$$C_v = \left[\begin{array}{cc} -(K_{pzs}^{\mathrm{elect}})^{-1} K_{pzs}^{\mathrm{elastelect}} & 0 \end{array}\right] \tag{27}$$

(where K_{pzs}^{elect} is the the partition of the matrix K_{pz}^{elect} corresponding to the sensors) and

$$C_w = \left[\begin{array}{cc} s^T & 0 \\ s_{rc}^T & 0 \\ s_{sr}^T & 0 \end{array}\right] \tag{28}$$

respectively. In this last equation, the subscripts sr and sc denote the output vectors for the source(s) and receiver(s) respectively (i.e. the equipment boxes here).

This model is in the standard form for controller design studies using any one of the standard techniques. The basic problem is to design the controller to suppress the effects of the disturbance vector f on the controlled output. In this paper, we consider linear quadratic optimal controller design - for H_∞ based design see [1]. Before such design studies are undertaken, however, it is essential to verify that the model of (26)-(28) is an adequate basis for such studies, i.e. we must verify the model as discussed briefly next with full details in [1, 3].

Model verification here is by comparing the results produced by the model (26)-(28) with those produced by standard FEM (ANSYS code [1]). To illustrate this method, consider the case where the panel is a simply supported aluminum plate of dimensions (length, breadth, and thickness respectively in mm) $304.8 \times 203.2 \times 1.52$ with 4 boxes mounted on it (for the panel properties and the locations of the boxes see the web site [4]). Box 1 is a passive equipment box (eg a box of electronic components), box 2 is a source of vibrations, and boxes 3 and 4 are receivers. Boxes 2, 3 and 4 are mounted on active suspensions, and box 1 is mounted on springs. The mass of each box is taken to be 0.5 kg equally divided between the mass of the enclosure and the mass of the resonator, and the rotational inertia of the boxes is $10^{-4} kg/m^2$. The four suspension springs are of stiffness $k = 10^6 N/m$ and the internal resonators, which are positioned at the center of each box to avoid coupling between linear (axial) and rotational (rocking) modes of the boxes, as have the same stiffness value.

A key point to note here is that the FE model has approximately 3500 dofs compared to 80 for the LRR model. Figure 2 shows a schematic view of the structure as modeled by the FEM. Comparisons of the results (a large range of sample results are given in [4]) obtained by the two models show that a very good agreement between them is present with only a slight frequency shift at high frequencies, which can be avoided by extending the model base for modeling panel displacements and refining the mesh used in the FE Model.

The mathematical model developed here is very flexible in terms of investigating the effects of different

input and output connections for vibration transmission reduction, eg minimization at the source(s), or receiver(s), or along the transmitting structure. In the work reported here we consider observer implemented state feedback design to minimize a standard linear quadratic cost function of the form

$$J = \int_0^\infty (w_{out}^T Q w_{out} + v_a^T R v_a)\, dt \qquad (29)$$

where the weighting matrices Q and R are symmetric positive semi-definite and symmetric positive definite respectively. For brevity, we do not repeat the details of the designs here. Instead, we focus on the interpretation of them in terms of the three strategies listed above and refer the reader to the web site [4] for complete details including the positions of the actuator and sensor, the excitation force, and the choice of and Q and R.

In the case of the structure investigated here, control along the transmission path, attempted using piezoelectric patches bonded onto the panel acting as actuators and sensors, did not give acceptable results. This is mainly due to the relatively low level of force which can be produced by the patch used as an actuator. In particular, the controller was only able to slightly reduce the amplitudes of the peaks in the frequency response corresponding to the first and third modes and it was not effective in reducing the response at other resonances. The reason for this is due to the position of the actuator patches which lie along a nodal line of most of the nodes and, in particular, nodes 2 and 4.

The situation does not improve if the controller has other signals available e.g. the displacements of the receivers, which confirms that the problem of this configuration lies in the position of the actuators. Better results can be obtained when the control is applied at the mechanical interface of the source or receiver, as described in turn next.

A: Control at source. In this case the control system drives (independently) the four suspensions of the equipment enclosure which generates the vibrations (source). The objective is to minimize the displacements and rotations of the two receivers. The signals available to the controller are numerous, and the option considered here is to use the displacements and rotations of the source as sensor signals. The controller design is based on a plant model which uses the first 4 by 4 modal shapes of the bare panel, and afterwards, the performance of the controlled structure is simulated by using a more accurate plant model (built using a 6 by 6 modal base). Figure 3 shows the vertical displacements of a receiver (which correspond to box 3 on the panel) with and without control.

: **Note:** In both Figures 3 and 4, the continuous line the displacement with no control action and the dashed line is the result of applying the feedback controller.

B: Control at receiver. The vibrations at the sensitive equipment can be reduced by acting on the equipment's suspensions. In this case the signals available to the control system are taken as the displacements and rotations of the receivers, and the controller drives the active suspensions of the receivers in order to minimize their displacements and rotations. The results (for the same numbers of modal shapes and bases) are reported in Figure 4. Note that, compared with the active control at source (Figure 3), this strategy allows a stronger reduction of the vibration level at the receivers location. Also this type of controller is relatively easy to implement because the sensors and actuators are located very close to each other.

Note that, even if the control strategies (A and B) presented in this paper are local, the panel plays an important role in the overall dynamics of the plant. The importance of a correct model of the panel in the global model of the plant, is highlighted by the fact that the plant may become unstable for small changes in the panel characteristics. As an example, the controller designed in the case A, which produces a stable controlled plant Figure 3, becomes unstable for a 5% change in the panel in the panel thickness.

4 CONCLUSIONS

This paper has used a Lagrange-Rayleigh-Ritz (LRR) approach to develop state space models of the dynamics of an equipment loaded panel on which to undertake the design of active control strategies based on feedback control schemes. The equipment enclosures have been modeled as rigid rectangular boxes mounted on a flexible panel. The enclosures have internal resonators to simulate internal dynamics and there is provision for rigid or flexible mounting elements to allow for active/passive suspensions. Piezoelectric patches are used as sensors and actuators on the panel and piezoelectric prisms are used for the box suspensions. A comparison of the results obtained, with those obtained by modeling the same system with the FE method, has established the validity and efficiency of the LRR approach to simulate the dynamics of this type of systems. The reduced size of this LRR model, in comparison with the FE model, makes it particularly suitable for investigations into the active control of vibrations, since it is able to capture the essential dynamics of the plant in a model of manageable size. Thus the LRR approach provides a convenient way of assessing various control algorithms and strategies.

References

[1] Aglietti, G. S., 1999, "Active Control of Microvibrations for Equipment Loaded Spacecraft Panels", PhD Thesis, University of Southampton, U.K.

[2] Aglietti, G. S., Gabriel, S. B., Langley, R. S., and Rogers, E., 1997, J. Acoustical Society of America, 102(4), 2158-2166.

[3] Aglietti, G. S., Langley, R. S., Rogers, E., and Gabriel, S. B., 2000, J. Acoustical Society of America, revised and re-submitted.

[4] URL http://wwww.isis.ecs.soton.ac.uk/ etar

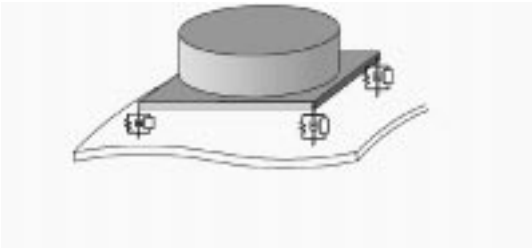

Figure 1:

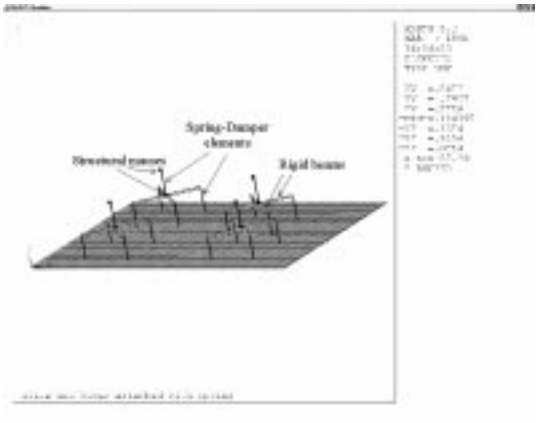

Figure 2:

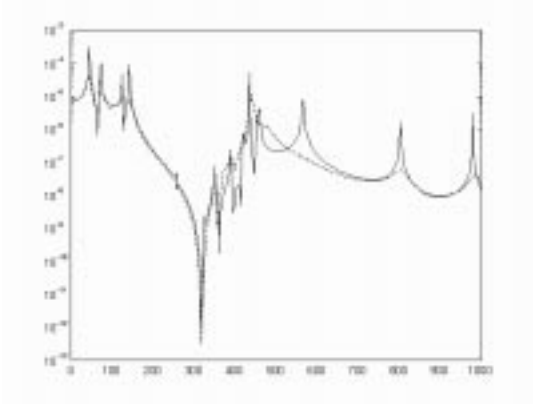

Figure 3:

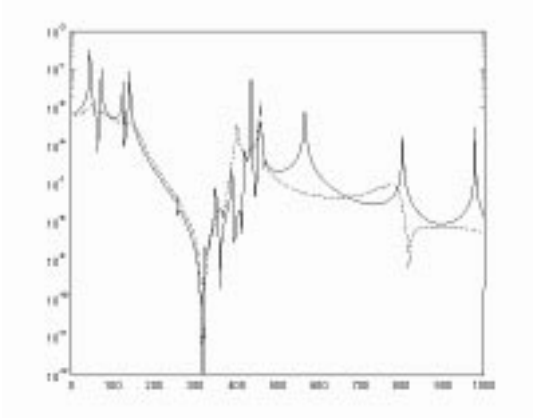

Figure 4: